THE JOURNAL OF BIOLOGICAL CHEMISTRY
Vol. 275, No. 29, Issue of July 21, pp. 22009–22013, 2000

Printed in U.S.A.

Domain Swapping in Human αA and αB Crystallins Affects Oligomerization and Enhances Chaperone-like Activity*

Received for publication, April 18, 2000, and in revised form, April 27, 2000
Published, JBC Papers in Press, April 28, 2000, DOI 10.1074/jbc.M003307200

L. V. Siva Kumar‡ and Ch. Mohan Rao§

From the Centre for Cellular and Molecular Biology, Hyderabad 500007, India

αA and αB crystallins, members of the small heat shock protein family, prevent aggregation of proteins by their chaperone-like activity. These two proteins, although very homologous, particularly in the C-terminal region, which contains the highly conserved "α-crystallin domain," show differences in their protective ability toward aggregation-prone target proteins. In order to investigate the differences between αA and αB crystallins, we engineered two chimeric proteins, αANBC and αBNAC, by swapping the N-terminal domains of αA and αB crystallins. The chimeras were cloned and expressed in *Escherichia coli*. The purified recombinant wild-type and chimeric proteins were characterized by fluorescence and circular dichroism spectroscopy and gel permeation chromatography to study the changes in secondary, tertiary, and quaternary structure. Circular dichroism studies show structural changes in the chimeric proteins. αBNAC binds more 8-anilinonaphthalene-1-sulfonic acid than the αANBC and the wild-type proteins, indicating increased accessible hydrophobic regions. The oligomeric state of αANBC is comparable to wild-type αB homoaggregate. However, there is a large increase in the oligomer size of the αBNAC chimera. Interestingly, swapping domains results in complete loss of chaperone-like activity of αANBC, whereas αBNAC shows severalfold increase in its protective ability. Our findings show the importance of the N- and C-terminal domains of αA and αB crystallins in subunit oligomerization and chaperone-like activity. Domain swapping results in an engineered protein with significantly enhanced chaperone-like activity.

α-Crystallin, a major lens protein having homology with small heat shock proteins (1–3), prevents aggregation of other proteins like a molecular chaperone (4). We had earlier shown that α-crystallin can prevent photo-aggregation of γ-crystallin, which may have relevance in cataractogenesis (5). By using various non-thermal modes of aggregation, it was shown that chaperone-like activity of α-crystallin is temperature-dependent. A structural perturbation above 30 °C enhances this activity severalfold (6, 7). In order to probe the molecular mechanism of the chaperone-like activity and its enhancement upon structural perturbation, we have been studying α-crystallin and its constituent subunits. Our recent study on the αA and αB homoaggregates showed that, despite high sequence homology, these proteins differ in their stability, chaperone-like activity, and the temperature dependence of this activity (8). This study also indicated different roles for the two proteins in the α-crystallin heteroaggregate in the eye lens and as separate proteins in non-lenticular tissues. Several investigators have introduced mutations in αA and αB crystallins to gain an insight into the structure-function relation (9–12). Derham and Harding in their recent review (13) list about 30 site-directed mutations from different laboratories. These mutations either result in some decrease or no change in the protective ability. It is interesting to note that point mutations in both αA and αB crystallin, R116C and R120G, respectively, result in significant loss of activity and are associated with human diseases (14–19).

Human αA and αB crystallins are coded by three exons (20, 21) and are thought to have arisen due to gene duplication. They share high sequence homology with the small heat shock proteins, which are found in all organisms, from prokaryotes to humans (22). αA and αB crystallins are constitutively expressed during normal growth and development. αA crystallin is expressed predominantly in the eye lens with small amounts being present in spleen and thymus (23), whereas αB crystallin is expressed not only in the eye lens, but also in several other tissues such as heart, skeletal muscle, placenta, lung, and kidney (24, 25). The main function of these proteins in the lens appears to provide transparency and prevent precipitation by binding to other aggregation-prone proteins. In the lens, αA and αB crystallins exist as heteroaggregates of approximately 800 kDa. Both the recombinant αA and αB crystallins exist as high molecular mass oligomeric proteins of approximately 640 and 620 kDa, respectively (26). The size of these proteins can vary a little depending on the pH and ionic strength, and they differ in their structure, function, tissue expression, and abnormal deposition in disease.

αB crystallin has a heat shock element upstream to the gene and is induced during stress (3, 28). Apart from maintaining lens transparency, its *in vivo* functions include interaction with intermediate filaments (29) and regulation of cytomorphological rearrangements during development (30). αB crystallin is hyperexpressed in neurological disorders such as Alzheimer's' disease, Creutzfeldt-Jacob disease, and Parkinson's disease (31–33).

The charged C-terminal domain is conserved in all the members of the small heat shock protein family, whereas the hydrophobic N-terminal domain is variable in length and sequence similarity (34). The N- and C-terminal domains are thought to form two structural domains with an exposed C-terminal extension (35). To investigate the role of the N-terminal domains in the differential structural and functional properties of human αA and αB crystallins, we have swapped their N-terminal domains coded by exon 1. A unique *Xmn*I restriction site at the beginning of the α-crystallin domain in a 20-

* This work was supported in part by the Department of Biotechnology, Goverment of India. The costs of publication of this article were defrayed in part by the payment of page charges. This article must therefore be hereby marked "*advertisement*" in accordance with 18 U.S.C. Section 1734 solely to indicate this fact.

‡ Recipient of a senior research fellowship from the University Grants Commission, Government of India.

§ To whom correspondence should be addressed. Tel.: 91-40-717-2241; Fax: 91-40-717-1195; E-mail: mohan@ccmb.ap.nic.in.

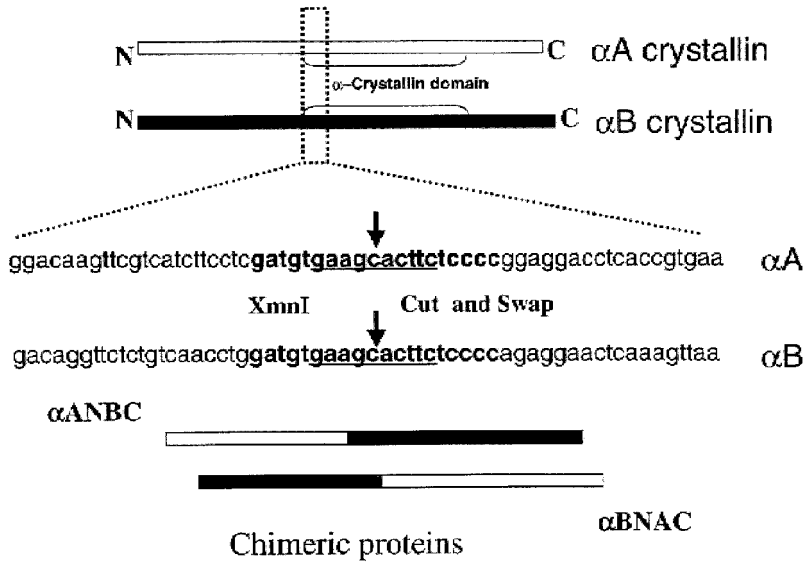

FIG. 1. **Schematic description of the design of chimeric constructs.**

nucleotide stretch in exon 2, with 100% sequence identity in human αA and αB crystallin genes, has been used to create chimeric proteins αANBC and αBNAC. We have used biophysical methods to study the structural and functional properties of wild-type αA and αB crystallins as well as the chimeras in order to get an insight into the effect of swapping and the role of the N-terminal domain in oligomerization and chaperone-like activity.

EXPERIMENTAL PROCEDURES

Construction of Human Chimeric αA and αB Crystallins

αANBC Chimera—The 235-base pair *Nde*I-XmnI fragment of pCR2.1-αA plasmid (16) was ligated to the 384-base pair XmnI-*Hin*dIII fragment of pCR2.1-αB plasmid (16) to generate chimeric coding region of αANBC. The αANBC chimera with *Nde*I-*Hin*dIII overhangs was then ligated to *Nde*I-*Hin*dIII-linearized expression vector pET21a (Novagen) to produce pET21a-αANBC.

αBNAC Chimera—The 247-base pair *Nde*I-XmnI fragment of pCR2.1-αB was ligated to the 446-base pair XmnI-*Hin*dIII fragment of pCR2.1-αA to generate the chimeric coding region of αBNAC. The αBNAC chimera with *Nde*I-*Hin*dIII overhangs was ligated to *Nde*I-*Hin*dIII-linearized pET21a to produce pET21a-αBNAC.

Sequencing of Human Chimeric αANBC and αBNAC Crystallins

Sequencing was done with T7 promoter primer using the dye terminator cycle sequencing kit (Perkin-Elmer) in an 3700 ABI automated DNA sequencer. The coding regions of both the αANBC and αBNAC chimeras were found to be mutationless with no change in the reading frame.

Overexpression and Purification of Human Wild-type and Chimeric αA and αB Crystallins

The expression plasmids (pET21a-αAwt, pET21a-αBwt, pET21a-αANBC, and pET21a-αBNAC) were transformed into competent *Escherichia coli* BL21(DE3) cells. Growth, induction, lysis of cells, and purification of chimeric proteins was done as described for recombinant wild-type αA and αB crystallins (26).

FPLC[1] Gel Permeation Chromatography

Multimeric sizes of the wild-type and chimeric proteins were evaluated on Superose-6 HR 10/30 prepacked column (dimensions: 10 × 300 mm, bed volume: 24 ml) with reference to high molecular mass standards (Sigma). Standards used were thyroglobulin (669 kDa), ferritin (440 kDa), and catalase (232 kDa).

Fluorescence Measurements

Intrinsic Fluorescence—Intrinsic fluorescence spectra of wild-type and chimeric proteins were recorded using a Hitachi F-4000 fluorescence spectrophotometer with the excitation wavelength of 295 nm. The excitation and emission band passes were set at 5 and 3 nm, respectively. Intrinsic fluorescence spectra were recorded using 0.2 mg/ml protein in 10 mM phosphate buffer, which was incubated at 37 °C for 10 min.

8-Anilino-1-naphthalenesulfonic Acid (ANS) Binding—Wild-type and chimeric proteins (0.2 mg/ml) in 10 mM phosphate buffer, pH 7.4, containing 100 mM NaCl were equilibrated at 37 °C in the sample holder of Hitachi F-4000 fluorescence spectrophotometer using a Julabo thermostated water bath for 10 min. To these protein samples, 20 μl of 10 mM ANS was added. Fluorescence spectra were recorded with an excitation wavelength of 365 nm. The excitation and emission band passes were 5 and 3 nm, respectively.

Circular Dichroism Studies

Circular dichroism spectra were recorded using a Jasco J-715 spectropolarimeter. All spectra reported are the average of 5 accumulations. Far- and near-UV CD spectra were recorded using 0.05- and 1-cm pathlength cuvettes, respectively.

Assay for Protein Aggregation

Chaperone-like activity of the wild-type and chimeric proteins was studied by the insulin aggregation assay (6, 36). The extent of protection by the wild-type αA and αB crystallins and the chimeric proteins was studied by incubating insulin (0.2 mg/ml) with various concentrations of the wild-type and chimeric proteins for 10 min at 37 °C. Aggregation was initiated by the addition of 20 μl of 1 M dithiothreitol (DTT) after the incubation.

RESULTS AND DISCUSSION

Construction and Expression of the Chimeric Human αA and αB Crystallins—Human αA and αB crystallin genes have a unique site for the restriction enzyme XmnI at the beginning of exon 2. A 20 nucleotide stretch at the *Xmn*I site in both αA and αB crystallins has 100% sequence identity. Swapping of the domains does not disturb the reading frame (Fig. 1). Since *Xmn*I site is slightly into the exon II, the excised N-terminal fragment has additional 15 amino acids. Of the 15 amino acids, 8 are identical and the rest are chemically conserved. Ligation of the N-terminal domain of αA crystallin with the C-terminal region of αB crystallin results in the chimeric polypeptide αANBC crystallin, which is 171 amino acids long. Similarly, the ligation of the N-terminal region of αB crystallin with C-terminal domain of αA crystallin creates polypeptide αBNAC crystallin that is 177 amino acids long. Henceforth, the chimeras are referred to as αANBC and αBNAC. Overexpression and purification of the chimeric proteins was carried out as described earlier for the wild-type proteins. The wild-type and chimeric proteins were purified to greater than 95% homoge-

[1] The abbreviations used are: FPLC, fast protein liquid chromatography; ANS, 8-anilino-1-naphthalenesulfonic acid; DTT, dithiothreitol.

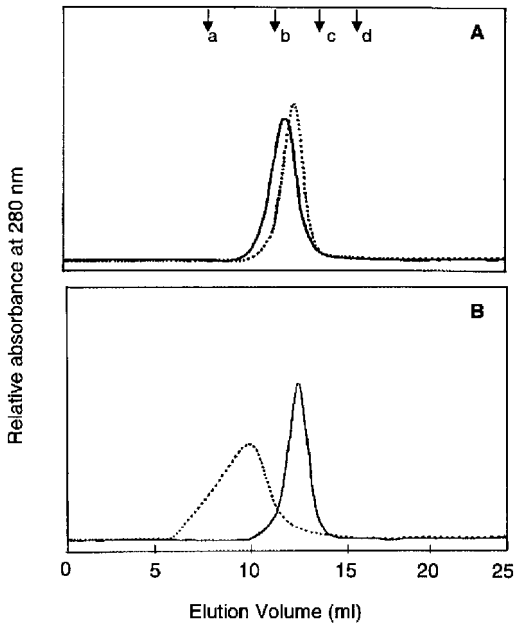

FIG. 2. **FPLC gel filtration profiles of wild-type αA and αB crystallins and chimeric proteins on a Superose-6 column.** *A*, wild-type αA crystallin (——) and wild-type crystallin αB (···). *B*, αANBC chimera (——) and αBNAC chimera (···). The void volume (*a*) and elution positions of thyroglobulin (669 kDa) (*b*), ferritin (440 kDa) (*c*), and catalase (232 kDa) (*d*) are also indicated.

neity, as judged by SDS-polyacrylamide gel electrophoresis (data not shown), and moved as ~20-kDa proteins as expected. Interestingly, when αANBC is eluted from a Mono Q ion exchange column with a 0–2 M NaCl gradient, it elutes at ~100 mM NaCl like the wild-type αB crystallin. On the other hand, αBNAC elutes at ~350 mM NaCl, similar to wild-type αA crystallin. The number of positively and negatively charged amino acids are identical in wild-type αA crystallin and αBNAC (Arg+Lys = 20; Asp+Glu = 25) and in wild-type αB crystallin and αANBC (Arg+Lys = 24; Asp+Glu = 25). A recently proposed model for α-crystallin suggests that the hydrophobic N-terminal domain is mostly buried in the oligomer (37). Thus, the C-terminal domain may largely determine the surface charge distribution of the proteins. This could be one of the reasons for the similarity in Mono Q elution profiles of wild-type proteins and chimeras that contain C-terminal regions identical to those of the wild-type proteins.

Superose-6 Gel Permeation Chromatography—To investigate the consequences of domain swapping on the molecular masses, chimeric and wild-type proteins were chromatographed on a FPLC Superose-6 gel filtration column (Fig. 2). The average molecular masses of wild-type αA and αB crystallins were observed to be ~640 and ~620 kDa, respectively. These sizes are consistent with earlier reports (16, 26). The chimera αANBC elutes at the same elution volume as that of wild-type αB with an apparent molecular mass of ~620 kDa. However the αBNAC chimera oligomerizes into large polydisperse aggregates, with species exceeding 2000 kDa. This finding shows an important difference in αA and αB crystallins. The αANBC chimera consisting of the N-terminal domain of αA crystallin and the C-terminal domain of αB crystallin still possesses the oligomer size of wild-type αA and αB crystallins. Thus, it appears that the N-terminal domain of αB crystallin can be replaced by the N-terminal domain of αA crystallin with no alteration in the oligomeric status. However, the N-terminal domain of αB crystallin in fusion with the C-terminal domain of αA crystallin forms very large aggregates, probably due to altered packing of the subunits with an increase in intersubunit interaction. This kind of increase in the oligomer size was earlier observed in the R116C mutant of αA crystallin (15). The monomer sizes of the proteins of the small heat shock protein family range from 12 to 43 kDa. Almost all members of this family multimerize to form large aggregates, ranging in size from 400 to 800 kDa with only one exception till date; sHSP 12.6 of *Caenorhabditis elegans*, which has the shortest N- and C-terminal domains, is monomeric (38). The N-terminal domain is variable in both length and sequence in the sHSP superfamily, which might be responsible for the varying multimeric sizes. Bova *et al.* (27) showed that sequential truncation from the N terminus of αA crystallin reduces oligomeric size. In the present study, the sequence length of the swapped N-terminal domain between αA and αB crystallin is similar, so the variation in sequence of this domain is likely to be responsible for the differential multimerization of the chimeric proteins.

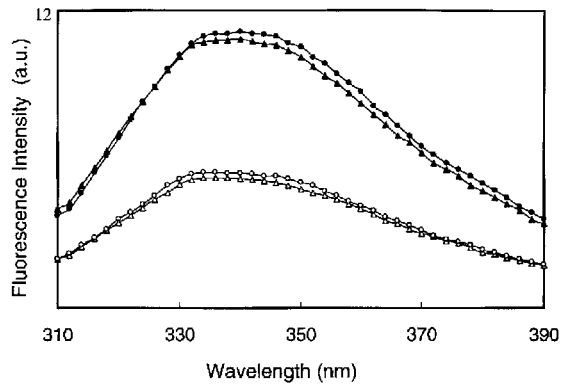

FIG. 3. **Intrinsic fluorescence spectra of wild-type αA crystallin (○), wild-type αB crystallin (●), αANBC (△), and αBNAC (▲).**

Intrinsic and ANS Fluorescence—The emission maximum of tryptophan is highly sensitive to solvent polarity and depends on the accessibility of tryptophan residues to the aqueous phase. Fig. 3 shows the intrinsic fluorescence spectra of wild-type and chimeric proteins. The intrinsic fluorescence spectra of the wild-type αB crystallin and αBNAC are similar. Both the tryptophans are present in the N-terminal domain, which are likely to be in a similar environment even after domain swapping. A slight blue shift, noticeable in the red region of the emission profile of αBNAC, compared with the wild-type αB crystallin suggests that the tryptophans in the chimera are marginally less solvent accessible. The intrinsic fluorescence spectra of the lone tryptophan of wild-type αA crystallin, which is present in the N-terminal domain, and αANBC are similar, indicating no alteration of the tryptophan environment in the chimeric αANBC protein with respect to the wild-type αA crystallin. Fig. 4 shows the spectra of ANS in the presence of wild-type and chimeric proteins. ANS fluorescence spectra show marked differences in emission intensity with no apparent change in emission maxima. The αANBC chimera binds the least amount of ANS among all the proteins compared. The αBNAC chimera, on the other hand, binds ANS several times more when compared with wild-type αB crystallin, wild-type αA crystallin, and αANBC chimera. This finding suggests that there are more hydrophobic regions accessible to ANS in the αBNAC chimera than in αANBC chimera. The molecular basis for this finding is not yet clear. However, the gel permeation chromatography data together with ANS fluorescence suggest that αBNAC might be forming a large porous oligomer.

Circular Dichroism Measurements of Chimeric αANBC and αBNAC Crystallins—Fig. 5 shows far-UV circular dichroism spectra of wild-type and chimeric proteins. CD spectra of wild-type αA and αB crystallins, shown in *panel A*, are comparable with the CD spectra of recombinant human αA and αB crys-

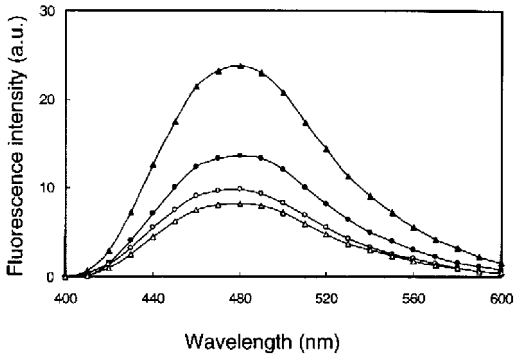

FIG. 4. **The normalized fluorescence emission spectrum of ANS bound to wild-type αA crystallin (○), wild-type αB crystallin (●), αANBC (△), and αBNAC (▲).**

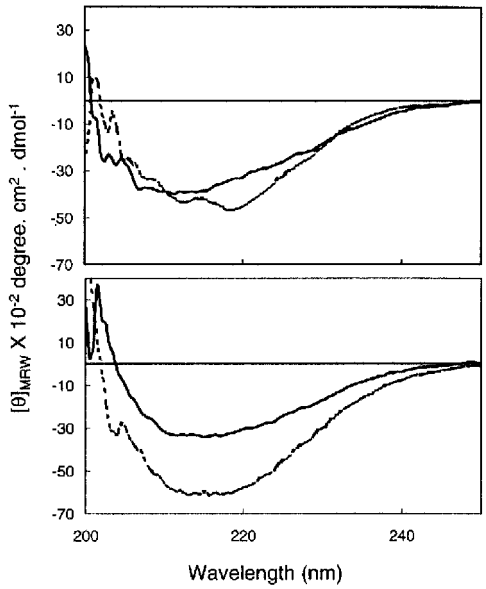

FIG. 5. **Far-UV CD spectra of wild-type αA and αB crystallins and chimeric proteins.** *A*, wild-type αA crystallin (···) and wild-type αB crystallin (——). *B*, αANBC (——) and αBNAC (···). The samples were prepared in 50 mM Tris-HCl buffer, pH 7.4, containing 100 mM NaCl and 1 mM EDTA.

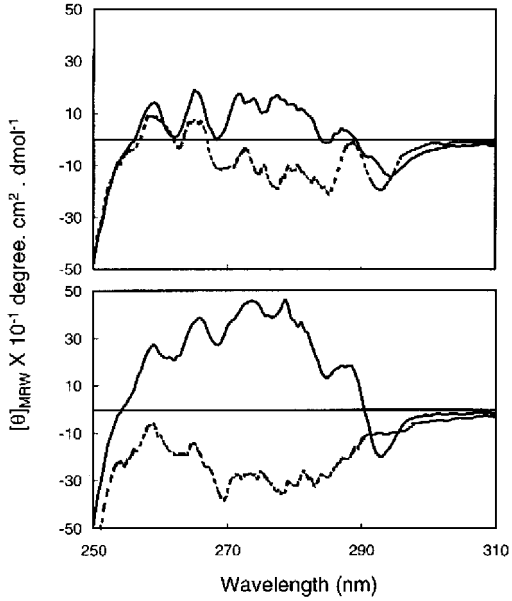

FIG. 6. **Near-UV CD spectra of wild-type αA and αB crystallins and chimeric proteins.** *A*, wild-type αA crystallin (···) and wild-type αB crystallin (——). *B*, αANBC (——) and αBNAC (···). The samples were prepared in 50 mM Tris-HCl buffer, pH 7.4, containing 100 mM NaCl and 1 mM EDTA.

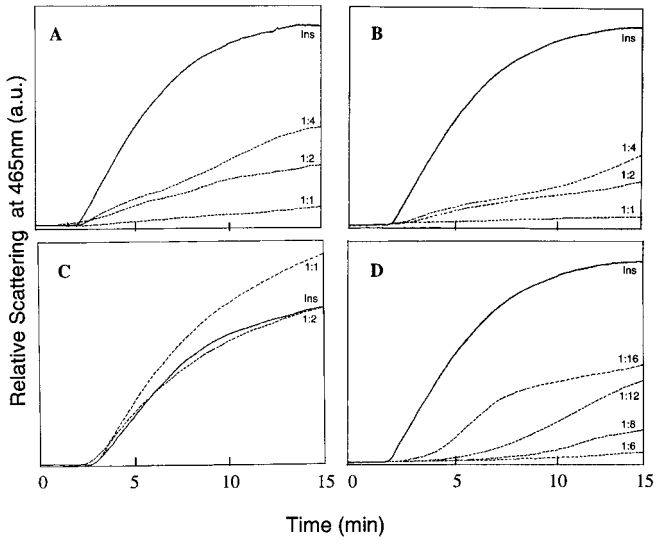

FIG. 7. **Chaperone-like activity of wild-type αA and αB crystallins and chimeric proteins.** *A*, effect of wild-type αA crystallin. DTT-induced aggregation of 0.2 mg/ml insulin alone (*Ins*) and in the presence of 1:1, 1:2, and 1:4 w/w wild-type αA crystallin:insulin, respectively. *B*, effect of wild-type αB crystallin. Panel shows aggregation of 0.2 mg/ml insulin alone (*Ins*) and in the presence of 1:1, 1:2, and 1:4 w/w wild-type αB crystallin:insulin, respectively. *C*, effect of αANBC chimera. Panel shows aggregation of 0.2 mg/ml insulin alone (*Ins*) and in the presence of 1:2 and 1:1 w/w αANBC:insulin, respectively. *D*, effect of αBNAC chimera. Panel shows aggregation of 0.2 mg/ml insulin alone (*Ins*) and in the presence of 1:6 1:8, 1:12, and 1:16 w/w αBNAC:insulin, respectively.

tallins reported earlier (15, 16, 26). Both the spectra show characteristic β-sheet protein profile as expected. Chimeric proteins also show β-sheet CD profiles. The CD spectrum of αANBC is comparable to the spectra of wild-type αA and αB crystallins. However, αBNAC shows increased ellipticity.

Near-UV CD spectra (Fig. 6) also show a similar trend. Spectra of wild-type αA and αB are comparable to earlier reported spectra for recombinant human αA and αB crystallins (15). The CD spectrum of the chimeric αANBC is comparable to that of αB crystallin with increased chirality for αANBC. The CD spectrum of αBNAC on the other hand is comparable to that of wild-type αA crystallin.

Domain swapping results in some change in secondary and tertiary structure of αANBC with observable change only in the secondary structure for αBNAC.

Chaperone-like Activity—Insulin B-chain aggregates in the presence of DTT. At 37 °C a 1:1 (w/w) ratio of wild-type αA and αB crystallin to insulin prevented this aggregation completely. At ratios of 1:2 and 1:4, aggregation was prevented to lesser extents, as shown in Fig. 7 (*panels A* and *B*). Interestingly, the chimera αBNAC showed enhanced chaperone-like activity. The initial scatter value for αBNAC chimera without insulin was very high. The large molecular size of αBNAC could be responsible for the high scatter. We had earlier observed a similar high initial scatter value for the R116C mutant of αA crystallin, which also forms a large aggregate (>2000 kDa) (16). The data were normalized to determine the protective ability of the αBNAC protein. At 37 °C complete protection was observed at a 1:6 w/w ratio of αBNAC to insulin. Significant protection was observed even at 1:8, 1:12, and 1:16 ratios of αBNAC to insulin (Fig. 7*D*). The αBNAC chimera shows 3–4-fold increase in the

chaperone-like activity compared with the wild-type proteins. αANBC, in contrast, shows complete loss of chaperone-like activity. A 1:2 (w/w) ratio of αANBC to insulin does not show any protective ability toward DTT-induced aggregation of insulin. Increasing the αANBC ratios to 1:1 and 2:1 w/w with respect to insulin does not show any increase in protection (Fig. 7*C*). In fact, αANBC promotes the aggregation process as observed by increased light scattering.

The swapped N-terminal domain (exon 1 encoded) is comparable in length between human αA and αB crystallins. There are some differences in the sequences in this region. One of the prominent differences is the increase in the number of proline residues. The N-terminal domain of αA crystallin contains 5 proline residues, whereas the same region for αB crystallin has 9 proline residues (two prolines in tandem). The swapping alters the number of proline residues in the chimeric proteins. αBNAC contains 9 prolines in its N-terminal domain, a gain of 4 prolines in comparison to the same region of wild-type αA crystallin. Far-UV CD spectrum shows some enhancement in the secondary structure. Whether the local secondary structural changes can alter the subunit topology and consequently intersubunit interactions remains to be investigated. Although we point out differences in the number of proline residues, there are other sequence variations, and marginal changes in predicted pI and the total length of the chimeric proteins. Clearly discernible changes are oligomeric status, accessible hydrophobic surfaces, and chaperone-like activity.

It is interesting to note that, despite being similar to wild-type αB crystallin in the aggregate molecular mass and circular dichroism spectra, the chimeric αANBC possesses no chaperone-like activity. The most important difference between the two chimeric proteins is the accessible hydrophobicity. ANS, a hydrophobicity probe, very clearly distinguishes the two chimeric proteins. We believe that the lack of accessible surface hydrophobicity, probably due to altered subunit packing in αANBC chimera, results in its loss of chaperone-like activity.

The enhanced chaperone-like activity of αBNAC chimera could be because of the exposure and availability of more hydrophobic surfaces when compared with the wild-type proteins. Increased ANS binding of the αBNAC chimera supports this possibility. We observed an increase in oligomeric size and chaperone-like activity in the case of the αBNAC chimera. However, the increase in size and enhancement of chaperone-like activity may not be necessarily correlated. The point mutation R116C in αA crystallin leads to increased oligomer size but results in significant loss of chaperone-like activity. Swapping the N-terminal domain between human αA and αB crystallins makes a more effective chaperone in the case of αBNAC chimera, whereas αANBC chimera loses its protective abilities completely. To the best of our knowledge, this is the first report where a 3–4-fold increase in chaperone-like activity is observed. This phenomenon may have a therapeutic significance in diseases occurring due to protein misfolding.

Acknowledgments—We thank Dr. T. Ramakrishna for critical reading of the manuscript and Shradha Goenka for useful discussions.

REFERENCES

1. Ingolia, T. D., and Craig, E. A. (1982) *Proc. Natl. Acad. Sci. U. S. A.* **79,** 2360–2364
2. de Jong, W. W., Leunissen, J. A. M., Leenen, P. J. M., Zweers, A., and Veersteeg, M. (1988) *J. Biol. Chem.* **263,** 5141–5149
3. Klemenz, R., Fröhli, E., Steiger, R. H., Schäfer, R., and Aoyama, A. (1991) *Proc. Natl. Acad. Sci. U. S. A.* **88,** 3652–3656
4. Horwitz, J. (1992) *Proc. Natl. Acad. Sci. U. S. A.* **89,** 10449–10453
5. Raman, B., and Rao, Ch. M. (1994) *J. Biol. Chem.* **269,** 27264–27268
6. Raman, B., Ramakrishna, T., and Rao, C. M. (1995) *FEBS Lett.* **365,** 133–136
7. Raman, B., and Rao, Ch. M. (1997) *J. Biol. Chem.* **272,** 23559–23564
8. Datta, S. A., and Rao, Ch. M. (1999) *J. Biol. Chem.* **274,** 34773–34778
9. Smulders, R. H. P. H., Merck, K. B., Aendekerk, J., Horwitz, J., Takemoto, L., Slingsby, C., Bloemendal, H., and de Jong, W. W. (1995) *Eur. J. Biochem.* **232,** 834–838
10. Andley, U. P., Mathur, S., Griest, T. A., and Petrash, J. M. (1996) *J. Biol. Chem.* **271,** 31973–31980
11. Plater, M. L., Goode, D., and Crabbe, M. J. (1996) *J. Biol. Chem.* **271,** 28558–28566
12. Muchowski, P. J., Wu, G. J. S., Liang, J. J. N., Adman, E. T., and Clark, J. I. (1999) *J. Mol. Biol.* **289,** 397–411
13. Derham, B. K., and Harding, J. J. (1999) *Prog. Retin. Eye. Res.* **18,** 463–509
14. Vicart, P., Caron, A., Guicheney, P., Li, Z., Prévost, M. C., Faure, A., Chateau, D., Chapon, F., Tomé, F., Dupret, J. M., Paulin, D., and Fardeau, M. (1998) *Nat. Genet.* **20,** 92–95
15. Bova, M. P., Yaron, O., Huang, O., Haley, D. A., Stewart, P. L., and Horwitz, J. (1999) *Proc. Natl. Acad. Sci. U. S. A.* **96,** 6137–6142
16. Kumar, L. V. S., Ramakrishna, T., and Rao, C. M. (1999) *J. Biol. Chem.* **274,** 24137–24141
17. Perng, M. D., Muchowski, P. J., van den IJssel, P., Wu, G. J., Hutcheson, A. M., Clark, J. I., and Quinlan, R. A. (1999) *J. Biol. Chem.* **274,** 33235–33243
18. Shroff, N. P., Cherian-Shaw, M., Bera, S., and Abraham, E. C. (2000) *Biochemistry* **39,** 1420–1426
19. Litt, M., Kramer, P., LaMorticella, D. M., Murphy, W., Lovrien, E. W., and Weleber, R. G. (1998) *Hum. Mol. Genet.* **7,** 471–474
20. Quax-Jeuken, Y., Quax, W., van Rens, G., Khan, P. M., and Bloemendal, H. (1985) *Proc. Natl. Acad. Sci. U. S. A.* **82,** 5819–5823
21. Ngo, J. T., Klisak, I., Dubin, R. A., and Piatigorsky, J. (1989) *Genomics* **5,** 665–669
22. de Jong, W. W., Caspers, G. J., and Leunissen, J. A. M. (1998) *Int. J. Biol. Macromol.* **22,** 151–162
23. Kato, K., Shinohara, H., Kurobe, N., Goto, S., Inaguma, Y., and Ohshima, K. (1991) *Biochim. Biophys. Acta* **1080,** 173–180
24. Bhat, S. P., and Nagineni, C. N. (1989) *Biochem. Biophys. Res. Commun.* **158,** 319–325
25. Dubin, R. A., Warwousek, E. F., and Piatigorsky, J. (1989) *Mol. Cell. Biol.* **9,** 1083–1091
26. Sun, T. X., Das, B. K., and Liang, J. J. N. (1997) *J. Biol. Chem.* **272,** 6220–6225
27. Bova, M. P., Mchaourab, H. S., and Fung, B. K. K. (2000) *J. Biol. Chem.* **275,** 1035–1042
28. Bennardini, F., Wrzosek, A., and Chiesi, M. (1992) *Circ. Res.* **71,** 288–294
29. Djabali, K., de Néchaud, B., Landon, F., and Portier, M., (1997) *J. Cell Sci.* **110,** 2759–2769
30. Scotting, P., McDermott, H., and Mayer, R. J. (1991) *FEBS Lett.* **285,** 75–79
31. Renkawek, K., Voorter, C. E. M., Bosman, G. J. C. G. M., van Workum, F. P. A., and de Jong, W. W. (1994) *Acta Neuropathol.* **87,** 155–160
32. Renkawek, K., de Jong, W. W., Merck, K. B., Frenken, C. W. G. M., Van Workum, F. P. A., and Bosman, G. J. C. G. M. (1992) *Acta Neuropathol.* **83,** 324–327
33. Renkawek, K., Stege, G. J., and Bosman, G. J. C. G. M. (1999) *Neuroreport* **10,** 2273–2276
34. De Jong, W. W., Leunissen, J. A. M., Voorter, C. E. (1993) *Mol. Biol. Evol.* **10,** 103–126
35. Wistow, G., (1985) *FEBS Lett.* **181,** 1–6
36. Farahbakhsh, Z. T., Huang, Q. L., Ding, L. L., Altenbach, C., Steinhoff, H. J., Horwitz, J., and Hubell, W. L. (1995) *Biochemistry* **34,** 509–516
37. Smulders, R. H. P. H., van Boekel, M. A. M., and de Jong, W. W. (1998) *Int. J. Biol. Macromol.* **22,** 187–196
38. Leroux, M. R., Melki, R., Gordon, B., Batelier, G., and Candido, E. P. M. (1997) *J. Biol. Chem.* **272,** 24646–24656